Proceedings of Montreal 2018
Global Power and Propulsion Forum
7th – 9th May, 2018
www.pps.global

GPPS-NA-2018-0161

The Role of Thermally Grown Oxide in the Failure Thermal Barrier Coatings for Gas Turbine Engine Applications

Vladimir Pankov
National Research Council Canada
Vladimir.Pankov@nrc-cnrc.gc.ca
Ottawa, Ontario, Canada

Prakash C. Patnaik
National Research Council Canada
Prakash.Patnaik@nrc-cnrc.gc.ca
Ottawa, Ontario, Canada

Kuiying Chen
National Research Council Canada
Kuiying.Chen@nrc-cnrc.gc.ca
State, Ottawa, Ontario, Canada

ABSTRACT

Thermal barrier coatings (TBCs) are widely used in gas turbine engines for propulsion and power generation to maximize engine operating temperature and fuel efficiency. TBCs comprise primarily three major components: the ceramic top coat, the intermetallic bond coat and a thin layer of a thermally grown oxide (TGO) formed at the bond coat/top coat interface. It was demonstrated that the TGO layer plays a critical role in determining the TBC life time with many TBC failure events occurring with its direct involvement. However, the actual mechanisms that govern TBC degradation and failure are still not fully understood in terms of the TGO role and the effects of its properties on the failure process. Stress analysis and TBC life time modelling were used in this study to demonstrate that the TGO morphology, its specific mechanical and thermal properties significantly affect the degradation modes and failure behaviour of the entire TBC system while the particular failure mechanisms differ depending on the ceramic top coat fabrication process. In this paper, the effect of changes in the TGO layer during thermal cycling has been theoretically investigated for TBC with top coats fabricated by atmospheric plasma spray and electron beam physical vapour deposition and the differences in their degradation and failure have been discussed.

INTRODUCTION

Thermal barrier coatings (TBCs), consisting of an yttria-stabilized zirconia (YSZ) top coat and a metallic bond coat (BC) deposited onto a superalloy substrate, are commonly used in combination with internal air cooling to protect hot section components of gas turbine engines such as combustion chambers, turbine nozzles, guide vanes and turbine blades against hot combustion gases. By lowering the temperature of the component due to their low thermal conductivity, these coatings enable higher engine operating temperatures thereby increasing engine fuel efficiency and extending the component life time (Beele *et al*., 1999; Padure *et al*., 2002). While the YSZ layer provides thermal insulation of the component, the role of the metallic bond coat is to enhance the adhesion of the YSZ layer to the metallic substrate and also provide its protection against high-temperature oxidation and corrosion (Chang-Jiu *et al*., 2012; Evans *et al*., 2001; Steinbrech and Basu, 2003).

A general understanding regarding TBC's failure is that in-plane biaxial compressive stresses are built up at the interface between the ceramic top coat and the bond coat during cooling from elevated to ambient temperatures because of their thermal expansion mismatch. The biaxial compressive stresses produce a tensile stress normal to the coating interface due to local tortuosity of the interface morphology. The tensile stress forces act on pre-existing flaws and defects causing crack nucleation and delamination in the TBC system constituents (Rabiei and Evans, 2000; Vaßen *et al*., 2001).

It is commonly believed that failure of TBC systems is largely attributed to changes occurring in a TGO layer naturally formed at the interface between the ceramic top coat and the aluminium-rich bond coat. In particularly, large stresses can develop with TGO layer thickening upon progressive oxidation of the bond coat (Magnus *et al*., 2004; Ranjbar-Far *et al*., 2010). Simultaneously, extensive cracks can nucleate at the sites where transient mixed oxides such as spinels form, leading to a reduced fracture toughness of the TGO layer (Liu *et al*., 2013; Tanaka *et al*., 2006). Based on the above mentioned failure mechanisms, various life models of TBCs have been proposed.

It has also been observed in various TBC cyclic testing studies that the failure mechanisms can differ significantly depending on the method of top coat fabrication (Padure *et al*., 2002). For example, for TBCs with YSZ top coat deposited by atmospheric plasma spray (APS), the delamination crack path is formed predominately at the TGO - top coat interface (Echsler *et al*., 2006; Trunova *et al*., 2008). For TBC systems with top coats produced by electron beam physical vapour deposition (EBPVD) on the surface of relatively flat bond coats delamination occurs predominantly at the TGO - bond coat interface (Echsler *et al*., 2006; Wen *et al*., 2006). It is believed that this is due to the difference in (i)

tortuosity of the initial interfaces formed during these two deposition methods and (ii) YSZ microstructures (splat-like versus columnar for APS and EBPVD, respectively) leading to different levels of thermals stresses in the TBC system constituent layers. Therefore, interface roughness is important parameter that needs to be taken into consideration when developing TBC life predicting models.

Vaßen *et al.* (Vaßen *et al.*, 2009) investigated the life of APS-TBC systems through examining a subcritical crack growth rate using the following equation:

$$\int_{a_0}^{a_f} \frac{da}{a^{m/2}} = \frac{A^* Y^m}{K_{IC}^m} \cdot \int_{t_0}^{t_f} \sigma(T)^m \, dt \qquad (1)$$

where $\sigma(T)$ is the residual stress acting on the APS ceramic top coat, m is an exponent parameter to be fitted to experimental data, a is the crack length in the top coat, K_{IC} is the fracture toughness of the top coat, T represents the temperature and t is the exposure time. In their stress model, the coating interface profile such as the BC roughness amplitude, the wavelength and TGO thickness were included in the stress evaluation. However, in their life model (Vaßen *et al.*, 2009), the fitting parameter $A^* Y^m / K_{IC}^m$ in Eq. (1) represented a constant independent of testing temperatures used during TBC thermal cycling. However, it is well known that stresses developed within the TBC system are strongly dependent on the cyclic testing temperatures.

In the present paper, temperature-dependent model parameters were identified and fitted to the test life data collected from the literature (Renusch *et al.*, 2008; Traeger *et al.*, 2003). A stress model was proposed and used to describe stress levels in the valleys of the top coat. The proposed model took into account a number of important factors such as the top coat-TGO coefficient of thermal expansion (CTE) mismatch, the top coat-TGO interface roughness, and the TGO layer thickness. The CTE mismatch-related strain was shown to be the main contributor to the residual stresses developed in the vicinity of the top coat/TGO interface at the end of the test cycle. The proposed model was able to reveal an inverse relationship between the stress and the TGO thickness. The stress model parameters were fitted to the 3-D Finite Element Analysis (FEA) stress calculations (Ahrens *et al.*, 2002), while the life model parameters were fitted to the existing burner rig test life data for various APS-TBC systems published in open literature (Renusch *et al.*, 2008; Traeger *et al.*, 2003).

METHODOLOGY

For an ideal flat coating interface, there is no residual stress normal to the top coat/bond coat interface. However, the typical top coat-bond coat interface in APS-TBCs is characterized by significant microscale waviness. The presence of the interface roughness in a coating redistributes the residual stress along the surface of individual undulations. As a result, at the location of a valley or peak, tensile stress is incurred due to the interfacial roughness, and this, in turn, could cause crack nucleation and subsequent propagation, eventually leading to the coating spallation. In the present paper, the life prediction of TBCs relies primarily on the roughness analysis of the coating interface between the top coat and the TGO layer (see Figure 1). To study residual stress development in TBCs upon cooling and its effect on crack nucleation and propagation in the coating, it is assumed that the coating exhibits a stress-free state during the high temperature dwell period of the thermal cycle. Upon cooling, a large tensile stress, normal to the top coat-TGO interface, develops at the peak locations of individual undulations providing favourable conditions for crack nucleation in a relatively thin TGO layer. Subsequent crack propagation proceeds along the top coat-TGO interface until inhibited at the valley of the undulation due to compressive stress. As thermal cycling continues, the TGO layer thickens at the crack sites due to oxygen propagation through the cracks followed by progressive oxidation of the bond coat. The compressive stress in the top coat in the direction normal to the top coat-TGO interface at the valley location attenuates, and at a certain thickness of TGO, it changes to the tensile one. This tensile stress will, in turn, promote fatigue crack nucleation at the valleys and crack propagation toward the peaks along the top coat-TGO interface. The ultimate spallation failure of the top coat occurs when these neighbouring cracks coalesce.

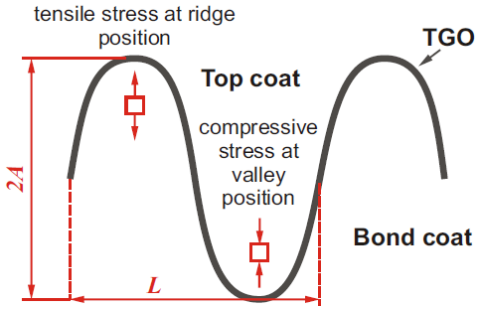

Figure 1 Proposed failure mechanism of APS-TBCs: as thermal cycling proceeds, the TGO layer thickens and stress inversion from compressive (shown in the figure) to tensile occurs at the valley locations of the top coat leading to crack nucleation at the valleys

STRESS MODEL

To calculate residual stress values in the top coat with an undulated top coat-TGO interface with a periodic wavy shape, we proposed the following stress model for the top coat at the valley location:

$$\sigma_{valley}(y) = -\alpha\Lambda\left\{(\alpha_{TGO} - \alpha_{TBC}) + (\alpha_{BC} - \alpha_{TGO})\left(1 - \beta\frac{d_{TGO}}{A}\frac{R}{y}\right)^3\right\}\left\{\left(\frac{R}{y}\right)^3 \qquad (2)$$

where α and β are two stress model parameters to be fitted to the 3-D FEA stress calculations (Ahrens *et al.*, 2002), $\Lambda = 4\kappa\mu_{TBC}\Delta T/(\kappa + 4\mu_{TBC}/3)$, $\mu_{TBC} = E_{TBC}/2(1+\upsilon_{TBC})$ and $\kappa = E_{TBC}/3(1-2\upsilon_{TBC})$. υ_{TBC} is the Poisson ratio of the top coat, ΔT is the temperature drop causing the CTE-induced residual stress. α_{TGO}, α_{BC}, α_{TBC} represent CTE values of the TGO layer, bond coat and top coat, respectively, at specific temperatures of these layers. d_{TGO} is the TGO thickness, A is the amplitude of the interfacial roughness, y is the valley

location of the top coat where the residual stress will be evaluated for crack propagation. R is the curvature radius at the valley location.

TOP COAT SINTERING AND GROWTH

Sintering of the top coat plays an important role in defining the remaining lifetime of TBC systems. The top coat sintering effect was also taken into account in the proposed stress model by an increase of the Young's modulus, E_{TBC} of the top coat when evaluating the crack growth rate using Eq. (1). The effect of sintering on the top coat Young's modulus can be described by (Vaßen *et al.*, 2009):

$$E_{TBC}(t) = \frac{\beta_s E^0_{TBC} E^\infty_{TBC}}{\beta_s E^0_{TBC} + E^\infty_{TBC} - E^0_{TBC}} \qquad (3)$$

$$\text{with } \beta_s = 1 + A_{\text{sint}} \exp\left(-\frac{E_{\text{sint}}}{\kappa_B T}\right) t^{p_s}$$

where κ_B is the Boltzmann constant, T is the temperature, and A_{sint}, E_{sint} and p_s are the sintering coefficient, sintering activation energy and sintering exponent of the top coat in APS-TBC, respectively. Although the model Eq. (2) describes the residual stress located at the top coat, it involves the effects of the TGO layer, bond coat and top coat through combined parameters such as the difference of CTEs between the TGO and the top coat, and also the CTE difference between the bond coat and the TGO, the TGO layer thickness as well as the elastic moduli of the bond coat and the top coat. In the present study, it is assumed that the TGO growth follows a parabolic law given by (Vaßen *et al.*, 2009):

$$d_{TGO} = A_{TGO} \exp\left(-\frac{E_{TGO}}{\kappa_B T}\right) t^{p_{TGO}} \qquad (4)$$

where A_{TGO}, E_{TGO} and p_{TGO} are the TGO layer growth rate coefficient, the TGO growth activation energy and the TGO growth exponent, respectively, with t to be an exposure holding time. As the interfacial profile is assumed to be approximately described by a sinusoidal curve, the curvature radius of the undulations is given by $R = L^2/4\pi^2 A$, where L represents the mean value of the wavelength. The valley location of y = 8 μm was selected according to the cross-sectional scanning electron microscopy (SEM) measurements of the top coat (Vaßen *et al.*, 2009).

LIFE PREDICTION PROCEDURE

By combining the described stress model and the subcritical crack growth formula Eq. (1), the predicted lifetime of APS-TBCs was evaluated numerically. The right hand side of Eq. (1) is an integral of the residual stress on the top coat from an initial time t_0 to t_f where the latter is the TBC life time till its failure, which needs to be determined. The left hand side of Eq. (1) is an integral of the crack length. It starts at a_0, an assumed half wavelength, increasing to a_f, the entire wavelength, which corresponds to the state when the top coat completely spalls from the bond coat. Eq. (1) can be interpreted as follows: the right hand side of Eq. (1) represents a driving force of the crack growth during the thermal cyclic process, while the left hand side of Eq. (1) describes the fatigue crack growth and propagation driven by the right side. When the crack length, a reaches the critical value, a_f, the cracks coalesce, resulting in a spallation of the entire top coat, which will define the TBC system failure time, t_f.

MODEL PARAMETERS

The results of cyclic burner rig testing of the APS-TBC system (Traeger *et al.*, 2003) were used to fit model parameters of Eq. (1). The basic test procedure consisted in rapid periodic heating of APS-TBC-coated disk shaped coupons for 5 min to the designed temperature in the 1200-1350°C range using a natural gas/oxygen burner while the coupon backside was simultaneously cooled by compressed air to maintain a temperature gradient through the sample (Traeger *et al.*, 2003). Then the sample was cooled to room temperature for 2 min by removing the burner and cooling the surface by compressed air. The cycles were repeated until failure of the sample occurred. It is believed that during the test the residual stress due to the CTE mismatch between the top coat and the substrate developed upon cooling to ambient. The value of the residual stress gradually grew with the increasing number of the test cycles leading to fatigue crack nucleation, propagation, linking and, eventually, coating spallation.

FEA-based calculations of stress distribution within the top coat of the TBC system were given by Ahrens *et al.* (Ahrens *et al.*, 2002). A basic procedure to implement the FEA stress calculations was based on the assumption of the stress-free state of the top coat at high temperature due to pronounced creep of the bond coat. The residual stress generated in the top coat upon cooling to ambient due to the CTE mismatch between the top coat and the substrate was calculated using elastic properties of materials at the ambient temperature. The thermal radial stress versus the TGO layer thickness at the valleys of the undulated top coat calculated using FEA (Ahrens *et al.*, 2002) is shown in Figure 2 together with the plotted curve obtained using the proposed stress model described by Eq. (2).

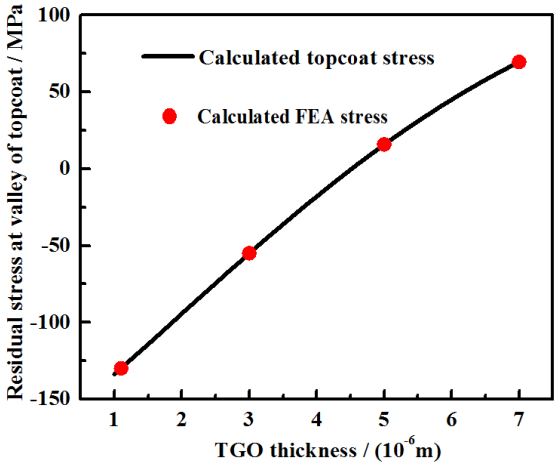

Figure 2 The calculated residual stress using Eq. (3) versus TGO thickness together with the stresses calculated by FEA (Ahrens *et al.*, 2002)

It can be seen from Figure 2 that the stress in the top coat changes from compressive to tensile when the TGO thickness exceeds a critical value h = 4.4 μm. This stress reversal phenomenon has been reported in several studies (Hsueg and Fuller, 2000; Schlichting *et al.*, 2003;). The amplitude of A = 7 μm and wavelength of λ = 65 μm were used to describe the interface roughness when fitting the residual stress model parameters α and β in Eq. (3). The fitted α and β are listed in Table 1. The parameters used to describe increase of the Young's modulus value due to sintering in the model (3) and the effect of the TGO layer thickness growth in model (4) are listed in Table 2. It is assumed that the residual stress model parameters α and β are temperature-independent, while the temperature-dependent characteristics of the life model are described by the life model fitting parameters A^*Y^m / K_{IC}^m in the subcritical crack growth formula Eq. (1).

Table 1 Stress model parameters in Eq. (2) and their related variables.

Parameters	A	R	y	α_{TGO}	α_{BC}
Abbreviation	Amplitude	Curvature radius	Valley location	CTE of TGO	CTE of BC
Value	7 μm	15.3 μm	8 μm	8×10-6K^{-1}	1.6×10-5K^{-1}
Parameters	α_{TBC}	α	β		
Abbreviation	CTE of TBC	Residual stress coefficient			
Value	1×10-5K^{-1}	0.174816	0.29585		

Table 2 The model parameters in TGO growth formula Eq. (4) and top coat Young's modulus sintering equation (3).

Parameters	d_{TGO}	A_{TGO}	E_{TGO}	p_{TGO}	T
Abbreviation	TGO thickness	TGO growth rate coefficient	TGO growth activation energy	TGO growth exponent	Temperature during a dwell period
Value		7.48×10^{-4} m/s	0.907 eV	0.25	1273.15K
Parameters	t	E_{TBC}	υ	E_{TBC}^{o}	E_{TBC}^{∞}
Abbreviation	exposure holding time	Young's modulus of TBC	Poisson ratio of TBC	Initial modulus of TBC	Bulk modulus of TBC
Value			0.33	20GPa	136GPa
Parameters	k_B	$A_{sin(t)}$	$E_{sin(t)}$	p_s	d_{TGO}^{c}
Abbreviation	Boltzmann constant	sintering coefficient	sintering activation energy	Sintering exponential coefficient	Critical TGO thickness
Value	1.38×10^{-23} J/K	2×10^{10} s^{-1}	3 eV	0.25	4.4 μm

In the fitting process, the model parameter A^*Y^m / K_{IC}^m was fitted to the test life data of the TBC system at specific temperatures. At different temperatures, the test life data were observed to vary and, as a result, the parameter A^*Y^m / K_{IC}^m also shows different values. It was found that the fitted A^*Y^m / K_{IC}^m parameter can be described using the following exponential formula:

$$\frac{A^*Y^m}{K_{IC}^m} = a_{fit}\exp(b_{fit}T) \qquad (5)$$

with two fitting parameters are a_{fit} =7.55×10^{-17} and b_{bit} =-0.16. In the study by Vaßen *et al.* (Vaßen *et al.*, 2009) the fitting parameter A^*Y^m / K_{IC}^m in the subcritical crack growth formula Eq. (1) was assumed as a constant although the life data was obtained at different temperatures. As a result, this may lead to large deviations in life prediction for APS-TBCs. As the parameter A^*Y^m / K_{IC}^m involves a combination of parameters including the top coat fracture toughness K_{IC}, this demonstrates that the top coat toughness K_{IC} is also a temperature-dependent property rather that a constant.

LIFE PREDICTION AND DISCUSSIONS

The TBC system used for the present life prediction study contained a vacuum plasma sprayed NiCoCrAlY bond coat characterized by a surface roughness R_a = (5.8±0.5) μm (Traeger *et al.*, 2003). This coating system was tested using a high cycle frequency burner rig. The presently selected wave amplitude A = 7 μm was close to the measured average roughness R_a. For this coating system, the fitted life model parameter A^*Y^m / K_{IC}^m in Eq.(1) reflected these specific coating materials as well as the test conditions. The proposed stress model and its parameters reflect the stress characteristics that show its dependence on the TGO layer thickness and, more importantly, transition of the residual stress in the top coat from compressive to tensile when exceeding a certain TGO thickness.

Using a temperature-dependent model parameter, the predicted APS-TBC life as a function of temperature in the range from 1273 K to 1348 K is shown in Figure 3. An exponential form was selected to describe this relationship:

$$t_f = 8.78\times10^{13}\exp(-0.02T) \qquad (6)$$

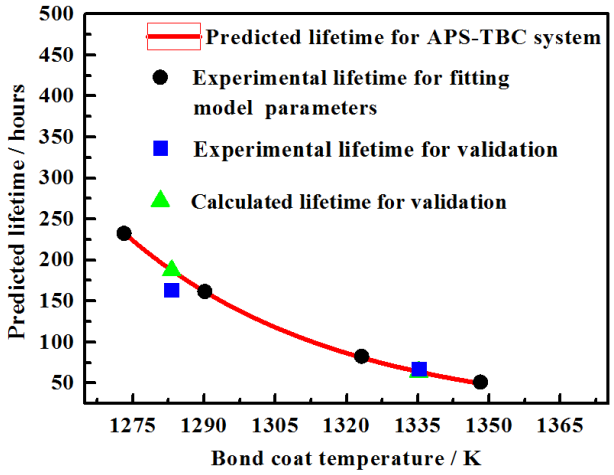

Figure 3 Predicted life versus the bond coat temperature. Four test life data (black solid circles) were used for model parameter A^*Y^m / K_{IC}^m fitting (Renusch *et al.*, 2008; Traeger *et al.*, 2003) and two test life data (blue squares) were used to validate the life model

As seen from the figure, the average life of the APS-TBCs decreases with increasing bond coat temperature. Four test life data (black solid circles) were used for model parameter A^*Y^m / K_{IC}^m fitting, while two test life data (blue squares) were used to validate the life model. According to Figure 3, the

life data (green triangles) predicted from the proposed model provide accurate fit with the test life data (black squares) at the specific temperatures illustrated in Figure 3 when using the temperature-dependent A^*Y^m/K_{IC}^m parameter.

EBPVD TBC Life Model

One of the most popular bond coats in TBC systems with the EBPVD top coat is Pt-modified aluminide. The predominant failure mode for such TBCs is through bond coat rumpling and deep penetration of the TGO into the bond coat while the bottom edge of the EBPVD top coat remains relatively flat (see Figure 4). Layer separation may occur at both the TGO/top coat and the TGO/bond coat interfaces. Based on the analysis of the rumpling effect, the stress intensity factor K at the crack tip of the top coat near the TGO was evaluated as (Mumm *et al*., 2001; Padure *et al*., 2002):

$$\mathrm{K} \approx \frac{E_{TBC}(dA/dN)}{2\sqrt{\pi}(1-\nu_{TBC}{}^2)\sqrt{L}}\left(\frac{L}{a}\right)^{3/2} N \qquad (7)$$

where E_{TBC} and ν_{TBC} stand for Young's modulus and Poisson's ratio of the top coat, respectively; dA/dN represents the rumpling rate of the TGO/top coat interface, N is the number of thermal cycles, a is the crack length within the top coat above the TGO shown in Figure 1. L represents the global wavelength shown in Figure 4, in which $L = 2d$.

In the present study, we assumed that the rumpling rate dA/dN of the TGO/top coat interface follows the same rumpling rate as the TGO/bond coat interface. Based on this assumption, the life model allows us to examine the influence of the interfacial rumpling amplitude on the life of EB-PVD TBCs.

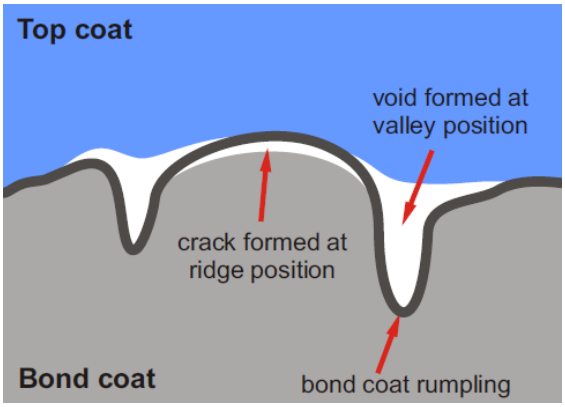

Figure 4 Ridges of the bond coat and voids of the top coat can be sites for crack nucleation in the EBPVD top coat due to rumpling of the bond coat

It can be seen from Eq. (7) that the stress intensity factor, K at the crack tip of the top coat does not depend on the properties of either the TGO layer or the bond coat. This K only involves properties of the top coat, although both the TGO and bond coat can show a strong effect on the stress distribution in the top coat. This effect can be taken into account by incorporating the measured temperature-process-dependent model parameters into the life model (Wen *et al*., 2006). To evaluate the TBC life, Eq. (7) can be rewritten as:

$$dA \approx \frac{\sqrt{\pi}(1-\nu_{TBC}{}^2)Ka^{3/2}}{E_{TBC}Nd}dN \qquad (8)$$

In the present TBC life evaluation study, the effect of sintering on the value of the top coat Young's modulus, E_{TBC} was also taken into consideration. Both E_{TBC} and wavelength d are dependent of the thermal cyclic temperature. Integrating Eq.(8) gives the maximum rumpling amplitude A in which failure occurs. It was observed through SEM analysis (Wen *et al*., 2006) that the TBC life was terminated almost at the same average rumpling amplitude of $A_f(T, N) \cong$ 4.2 μm for the coatings tested at three different temperatures. This independence of the average rumpling amplitude value on the temperature was applied in the present study to the TBC life evaluation. The upper-value in the integral of Eq. (8) on the left side was chosen in the study as 4.2 μm and the life cycle N_f was determined numerically.

The Fitting Model Parameters

The life data of furnace cyclic testing (FCT) of EBPVD TBCs deposited on the Pt-modified NiAl bond coat (Wen *et al*., 2006), were applied to predict TBC life using Eq. (8). The rumpling amplitude, A of the bond coat was used as a geometrical parameter describing the mean value of the rumpling amplitude of imperfections. In the study by Wen *et al*., the TGO/bond coat interface profiles at different exposure period during thermal cycling were selected from the cross-sectional SEM micrographs from TBCs tested at 1151°C, 1121°C and 1100°C, respectively. The results show that the amplitude of rumpling increases with the number of thermal cycles and the cycling temperature. A detailed analysis of the rumpling was conducted by evaluating a root mean square (RMS) value of rumpling amplitude of the interface profiles. It was clearly seen that the rumpling rate increases with the cycling temperature. The rumpling amplitude, A can be defined and calculated as (Tolpygo *et al*., 2004):

$$A = \sqrt{2}RMS \qquad (9)$$

A recompilation of data for the rumpling amplitude, A is presented in Figure 5 at three cycling temperatures: 1100°C, 1121°C and 1151°C. By fitting the rumpling amplitude, A to the temperature-process-dependent data, A was described as a function of thermal cycles N,

$$A = \sqrt{2}(RMS_{slope}N + RMS_{\mathrm{int}})\times 10^{-6} \qquad (10)$$

where the parameters RMS_{slope} and RMS_{int} were fitted to the testing data (Wen *et al*., 2006) as a function of temperature T in the following forms: $RMS_{slope} = 3.559\times 10^{-25}\exp(0.03635T)$ and $RMS_{\mathrm{int}} = -0.01032T + 15.7$.

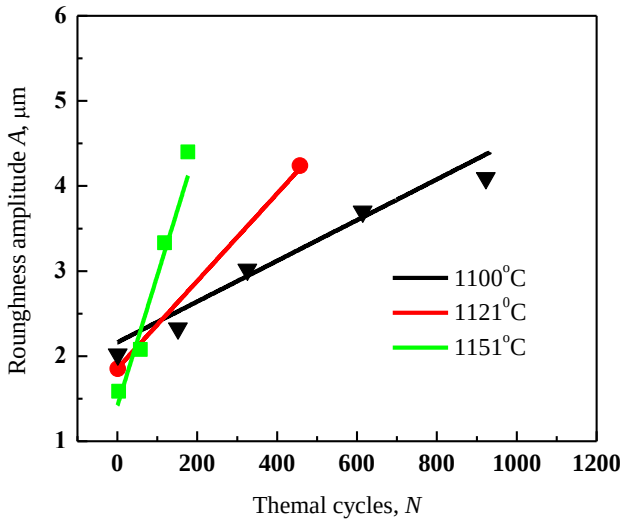

Figure 5 Bond coat rumpling (roughness) amplitude, *A* used in the lifetime prediction model. An increase of rumpling gradient was observed with increasing cycling temperature (Wen *et al*., 2006)

It was observed experimentally that the YSZ top coat of EB-PVD TBCs experience considerable sintering during a prolonged high temperature exposure, which consequently leads to an increase in the Young's modulus of the top coat as a result of a closure of vertical inter-columnar pores (Zhao *et al*., 2006). The increase of the Young's modulus has a significant effect on the preferential TBC failure mode and its life. In the present paper, the increased in-plane Young's modulus values measured by Zhao *et al.* as a function the TBC exposure time period were used to predict the life of TBCs using the model proposed by Vaßen *et al*. (Vaßen *et al*., 2009). The sintering model parameters A_{sint}, E_{sint} and n for the EB-PVD TBC top coat were obtained by fitting the model to the temperature-dependent Young's modulus data obtained by Zhao *et al*..

It was suggested by Wen *et al*. (Wen *et al*., 2006),that the rumpling wavelength *L*, describing the distance between individual undulations formed at the TGO/bond coat interface, plays an important role in determining life and failure modes in TBCs. It was demonstrated that a power spectrum of spacing between the individual inward displacements can be obtained using Fast Fourier Transform (FFT) and RSM analyses. The present study used these measured data to fit the wavelength, *L* as a function of the number of cycles calculated at specific temperatures, as shown in Figure 6. The mean curvature radius R_M, measured at the bond coat/TGO interface from the cross section of specimens at specific stages during thermal cycles was used to estimate the size of local imperfections.

For the APS-TBC system, a sinusoid-like profile of the TGO/bond coat or TGO/top coat interface was assumed and a sinusoidal function was used to describe such an interface. In the failure analysis and life prediction of these APS-TBC systems, the shape parameters, such as the amplitude, *A*, the wavelength, *L*, and their ratios, *A/L*, were incorporated in the models to calculate stresses at different coating layers or interfaces. However, in the failure analysis of EBPVD TBCs with Pt-modified β-NiAl as a bond coat, the TGO/bond coat or TGO/top coat interface is initially much flatter than that in the APS-TBC systems. Although the wavelength, *L* was still used in this study to describe the EBPVD TBC interface profile, it cannot be used to estimate the local stress at specific coating layers or interfaces. It is believed that no relationship exists between the global wavelength, *L* and local stresses in EBPVD TBC systems during their thermal cycling.

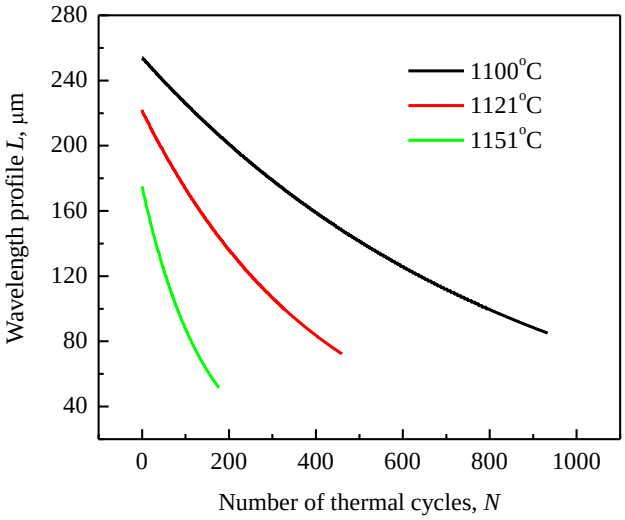

Figure 6 Calculated global wavelength, L as a function of the number of thermal cycles at three selected temperatures

Life Prediction Results

Although Eq. (8) was used to evaluate the rumpling amplitude, *A* versus the number of thermal cycles, *N*, this equation can also be applied to estimate the life of TBCs at specific temperatures. For example, the left side of Eq. (8) can be calculated through the integral by using the fitted parameter *A* based on Eq. (10). The integral of the right side of Eq. (8) can be evaluated using the Young modulus and wavelength values for the case of sintered top coat reported by Zhao et al. (Zhao *et al*., 2006). These fittings can be implemented using the furnace cyclic testing data presented by Wen *et al*. (Wen *et al*., 2006) at 1151°C, 1121°C and 1100°C. The factor $\sqrt{\pi}(1-\upsilon_{TBC}{}^2)K_{IC}^{TBC}a^{3/2}$ in the right side of Eq. (8) can be derived using the fitted parameters $A(N, t)$, E_{TBC} and $d(N, t)$. This temperature-dependent factor can be described by the following Gaussian-type function:

$$\sqrt{\pi}(1-\upsilon_{TBC}{}^2)K_{IC}^{TBC}a^{1.5} \approx 1\Big/\left\{1594\exp\left[-\left(\frac{\mathrm{T}-1419}{402.7}\right)^2\right]\right\}, \quad (11)$$

where the bond coat temperature, *T* was used as a reference temperature. Using the fitted model parameters in Eq. (11), the life prediction of the TBC system with the EBPVD top

coat and Pt-modified NiAl bond coat was conducted for the temperature range from 1100°C to 1151°C.

Figure 7 shows the calculated TBC life along with the FCT results. Upon obtaining the fitting factor $\sqrt{\pi}(1-\upsilon_{TBC}{}^2)K_{IC}^{TBC}a^{3/2}$, using the Eq. (7) and applying the condition A_f (T, N) = 4.3 μm in Eq.(11), the TBC life, N_f has been numerically obtained, as shown in the figure.

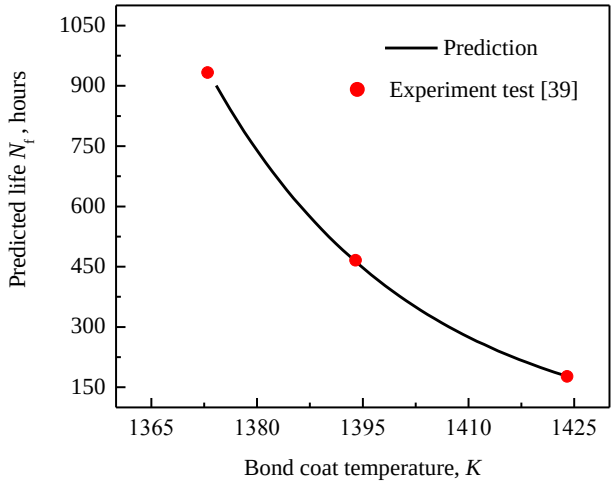

Figure 7 Predicted TBC life, N (in hours) as a function of bond coat temperature. Experimental furnace cycling test results obtained by Wen et al. (Wen et al., 2006) are shown with dots

CONCLUSIONS

Life prediction of APS-TBCs has been performed using a developed residual stress model fitted using published experimental data on burner rig cyclic testing of real TBC systems. The proposed stress model takes into account elastic and thermal physical properties of the TGO, bond coat and top coat. The model also uses geometric characteristics of the TGO/bond coat and TGO/top coat interfaces. Some of the stress model parameters were fitted to the experimental stress data obtained using FEA calculations. Temperature-dependent model parameters controlling crack propagation were obtained by fitting the model to the burner rig test data of APS-TBC systems. The APS-TBC life prediction was conducted by using temperature-dependent model parameters and the capability of the model for APS-TBC life prediction was largely improved by combining stress integrals with a critical time for the residual stress sign inversion.

Temperature-process-dependent model parameters were fitted and used in failure analysis and life prediction of TBCs with the EB-PVD top coat and the Pt-modified NiAl bond coat deposited on Ni-base single crystal superalloy substrates. In the failure analysis and life prediction of these TBCs, the maximum average rumpling amplitude of the bond coat/TGO interface, *A*, was used as a failure criterion. Model verification was performed at three exposure temperatures and the validity of the developed model was demonstrated by showing that high exposure temperatures lead to a shorter TBC life with the calculated numbers well matching with the published experimental data on furnace cyclic testing of similar TBCs. In the conducted life evaluation analysis, the experimentally determined temperature-dependent thickness of the TGO layer, the interfacial roughness, elastic moduli of constituent coatings and their coefficients of thermal expansion were applied in the developed TBC life model. The global wavelength associated with interface rumpling and its radius curvature was found to play an important role in life evaluation of this type of TBCs.

ACKNOWLEDGMENTS

This research work was supported by the Air Defense Systems Program of the National Research Council Canada, and the Natural Sciences and Engineering Research Council of Canada.

REFERENCES

Ahrens M., Vaβen R., and Stöver D. (2002). Stress distributions in plasma-sprayed thermal barrier coatings as a function of interface roughness and oxide scale thickness. Surface and Coatings Technology 161 (1), 26-35.

Beele W., Marijnissen G., and van Lieshout A. (1999). The evolution of thermal barrier coatings - status and upcoming solutions for today's key issues. Surface & Coatings Technology 120, 61-67.

Chang-Jiu Li, Yong Li, Guan-Jun Yang, and Cheng-Xin Li (2012). A novel plasma-sprayed durable thermal barrier coating with a well-bonded YSZ interlayer between porous YSZ and bond coat. Journal of Thermal Spray Technology 21 (3), 383-390.

Echsler H, Shemet V., Schutze M, Singheiser L., and Quadakkers W.J. (2006). Cracking in and around the thermally grown oxide in thermal barrier coatings: A comparison of isothermal and cyclic oxidation. J. Mater. Sci. 41 (4), 1047-1058.

Evans A. G, Mumm D. R. Hutchinson J. W, Meier G. H, and Pettit F. S. (2001). Mechanisms controlling the durability of thermal barrier coatings. Progress in Materials Science 46 (5), 505-553.

Hsueg C. H. and Fuller E. R. (2000). Analytical Modeling of Oxide Thickness Efforts on Residual Stresses in Thermal Barrier Coatings. Scripta mater. 42 (8), 781-787.

Liu D., Seraffon M., Flewitt P. E. J., Simms N. J., Nicholls J. R., Rickerby D. S. (2013). Effect of substrate curvature on residual stresses and failure modes of an air plasma sprayed thermal barrier coating system. Journal of the European Ceramic Society 33 (15-16), 3345-3357.

Magnus J. and Brodin H. (2004). Crack initiation and propagation in air plasma sprayed thermal barrier coatings, testing and mathematical modelling of low cycle fatigue behaviour. Materials Science & Engineering A 379 (1-2), 45-57.

Mumm D. R., Evans A. G. and Spitsberg I. T. (2001), Characterization of a cyclic displacement instability for a thermally grown oxide in a thermal barrier system. Acta Mater. 49 (12), 2329-2340.

Padure N. P., Gell M., and Jordan Eric E. H. (2002). Thermal barrier coatings for gas-turbine engine applications. Science 296 (5566), 280-283.

Rabiei A. and Evans A. G. (2000). Failure mechanisms associated with the thermally grown oxide in plasma-sprayed thermal barrier coatings. Acta Mater. 48 (15), 3963-3976.

Ranjbar-Far M., Absi J., Mariaux G., and Dubois F. (2010). Simulation of the effect of material properties and interface roughness on the stress distribution in thermal barrier coatings using finite element method. Materials and Design 31 (2),.772–781.

Renusch D., Schorr M., and Schütze M. (2008). The role that bond coat depletion of aluminum has on the lifetime of APS-TBC under oxidizing conditions. Materials and Corrosion 59 (7), 7-15.

Schlichting K. W., Padture N. P., Jordan N. P., and Gell M. (2003). Failure modes in plasma-sprayed thermal barrier coatings. Materials Science and Engineering A 342 (1-2) 120-130.

Steinbrech R. W. and Basu D. (2003). Ceramic based thermal barrier coating (TBC) for gas turbine application: Elastic behaviour of plasma sprayed TBC. Transactions of the Indian Ceramic Society 62 (4), 192-199.

Tanaka M., Hasegawa M., and Kagawa Y. (2006). Detection of micro-damage evolution of air plasma-sprayed Y_2O_3-ZrO_2 thermal barrier coating through TGO stress measurement. Materials Transactions 47 (10), 2512-2517.

Tolpygo V. K., Clarke D. R., and Murphy K. S. (2004). Evaluation of interface degradation during cyclic oxidation of EB-PVD thermal barrier coatings and correlation with TGO luminescence. Surface & Coatings Technology 188-189, 62–70.

Traeger F., Ahrens M., Vaßen R., and Stöver D. (2003). A life time model for ceramic thermal barrier coatings. Materials Science and Engineering A358 (1-2), 255-265.

Trunova O., Beck T., Herzog R., Steinbrech R. W., Singheiser L. (2008). Damage mechanisms and lifetime behavior of plasma sprayed thermal barrier coating systems for gas turbines—Part I: Experiments. Surface and Coatings Technology 202 (20) 5027-5032.

Vaßen R., Kerkhoff G., and Stöver D. (2001). Development of a micromechanical life prediction model for plasma sprayed thermal barrier coatings. Materials Science and Engineering A303 (1-2), 100–109.

Vaßen R., Giesen S., and Stöver D. (2009). Lifetime of plasma-sprayed thermal barrier coatings: Comparison of numerical and experimental results. Journal of Thermal Spray Technology 18 (5-6), 835–845.

Wen M., Jordan E. H., and Gell M. (2006). Effect of temperature on rumpling and thermally grown oxide stress in an EB-PVD thermal barrier coating. Surface & Coatings Technology 201 (6), 3289-3298.

Zhao X., Wang X., and Xiao P. (2006). Sintering and failure behaviour of EB-PVD thermal barrier coating after isothermal treatment. Surface & Coatings Technology 200 (20-21), 5946-5955.